Utilization of Cellulose Nanofibrils as a Binder for Particleboard Manufacture

Ezatollah Amini,[a] Mehdi Tajvidi,[a,*] Douglas Jerome Gardner,[b] and Douglas Wayne Bousfield [c]

Cellulose nanofibrils (CNF) were investigated as a binder in the formulation of particleboard (PB) panels. The panels were produced in four different groups of target densities with varying amounts of CNF binder. The produced panels were then tested to determine the modulus of rupture (MOR), modulus of elasticity (MOE), internal bond (IB), water absorption (WA), and thickness swelling (TS) properties. Density gradients through the thickness of the panels were evaluated using an X-ray density profiler. The effect of drying on the strength development and adhesion between CNF and wood particles (WP) was investigated, and the effect of surface roughness on the wood-CNF bonding strength was evaluated through lap shear testing and scanning electron microscopy. It was found that at lower panel densities, the produced samples met the minimum standard values recommended for particleboard panels. Medium-density panels met the standard levels for IB, but they did not reach the recommended values for MOR and MOE. The possible bonding mechanism and panel formation process are discussed in light of microscopic observations and the results of lap shear tests were presented.

Keywords: Cellulose nanofibrils; Binder; Particleboard; No-added formaldehyde

*Contact information: a: Laboratory of Renewable Nanomaterials, School of Forest Resources and Advanced Structures and Composites Center, University of Maine, Orono, ME 04469 USA; b: School of Forest Resources and Advanced Structures and Composites Center, University of Maine, Orono, ME 04469 USA; c: Department of Chemical and Biological Engineering, University of Maine, Orono, ME 04469 USA; *Corresponding author: mehdi.tajvidi@maine.edu*

INTRODUCTION

Particleboard is a wood composite panel typically manufactured from discrete wood particles combined with a resin or binder under heat and pressure. The resins used in particleboards are mostly made up of formaldehyde-based adhesives, such as urea-formaldehyde (UF) and, to a lesser extent, phenol-formaldehyde (PF) resin (Jambrekovi *et al.* 2006). The major concern associated with these resins is the emission of formaldehyde (Christensen *et al.* 1981), which has been proven to be carcinogenic. Over the past years, several approaches have been taken to reduce formaldehyde emissions from wood-based panels. This includes using liquefied wood (LW), wood meal of black poplar liquefied with a mixture of glycerol and sulfuric acid by heating, for the modification of phenol-formaldehyde (Antonovic *et al.* 2010), organosolv lignin dispersion to partially replace the solids content in a liquid phenol-formaldehyde (Seyno *et al.* 1996), hydrogen peroxide as a catalyst in the hardening process of urea-formaldehyde (Elbert 1995), low formaldehyde emission acrylic resin (Amazio *et al.* 2011), and pulp and paper secondary sludge as a urea-formaldehyde co-adhesive (Xing *et al.* 2013). A number of studies focused on the

replacement of formaldehyde-based resins with other binders such as epoxidized vegetable oils (Sivasubramanian *et al.* 2009; Tasooji *et al.* 2010), soy-based adhesives (Prasittisopin and Li 2010), tannins and lignin from pulp mill residues (Bertaud *et al.* 2012), and polymeric diphenylmethane diisocyanate (pMDI) (Tongboon *et al.* 2002).

Cellulose nanomaterials that are mainly available in the forms of cellulose nanofibrils (CNF), cellulose nanocrystals (CNC), and bacterial nanocellulose (BC), have attracted considerable interest attributed to the possibility of making strong, light, and biodegradable products from an abundant renewable resource. Some review articles have summarized the applications of these novel materials (Hubbe *et al.* 2008; Siró and Plackett 2010; Klemm *et al.* 2011; Moon *et al.* 2011; Dufresne 2012; Charreau *et al.* 2013; Gardner *et al.* 2013; Chirayil *et al.* 2014; Oksman *et al.* 2016). Cellulose nanomaterials are produced *via* aqueous suspensions with low consistency, which limits the applications of these materials as additives in systems where dry materials are required. These additive applications also generally consume small amounts of nanocellulose. With the current decline in the demand for pulp and paper worldwide (Ince 1999; Prestemon *et al.* 2015), finding large-scale applications in which these new materials can be utilized is critical for commercialization purposes.

Using cellulose nanomaterials in their original aqueous state provides a number of advantages; there is no need to dry the material prior to the production of the final product, thereby saving energy. It is possible to preserve the nanoscale dimensions in the final product and take advantage of the high reinforcement capacity of such materials, and it provides the opportunity to use higher amounts of nanocellulose in the product being made. Efforts have been made recently to use CNF as a binder in the formulation of the wood flour boards (Kojima *et al.* 2013, 2015), but these studies have been limited in scope and do not provide information on the bonding mechanisms. Veigel *et al.* (2012) utilized CNF as an additive in the formulation of formaldehyde-based adhesives of particleboards and oriented strand boards to improve their mechanical properties. Some recent study has been done to use 2,2,6,6-tetramethylpiperidine-l-oxyl (TEMPO) mediated CNF as a reinforcing agent in the manufacture of fiberboards from corn thermomechanical fibers (Theng *et al.* 2015).

This paper is focused on the manufacturing of particleboard panels using CNF that is produced through a refining process as a sole binder. Recent work at the University of Maine has shown that the use of CNF as a binder for the production of particleboard is feasible (Bilodeau and Bousfield 2014; Tajvidi *et al.* 2016). The goal of this study was to evaluate the technical feasibility of producing particleboard panels using CNF as the binder. We present the first complete set of data and analysis as well as efforts made to understand adhesion mechanisms and the strength development involved in such novel systems.

EXPERIMENTAL

Materials

Southern pine wood particles (WP) with an average length of 3.8 mm (aspect ratio of 3.3) and an average moisture content of 7% were supplied by Georgia-Pacific Thomson Particleboard (Thomson, GA, USA). A CNF slurry (containing 3% wt. cellulose nanofibrils) was used as the binder. The CNF was a product of the University of Maine's Process Development Center, which was produced *via* mechanical refining of bleached

softwood kraft pulp. The physical form of the 3 wt.% CNF slurry along with a transmission electron microscopy (TEM) image are shown in Fig. 1. While there are a large number of fibers that are 50 nm in thickness (Fig. 1), a number of fiber fragments or cell wall material in the CNF slurry is still present that have a length scale of a few microns. Polycup™ 5233, formerly known as Kymene®, (30% solids, received from Solenis LLC (Wilmington, DE, USA)) was used in some of the formulations as a formaldehyde-free, water-based, crosslinking agent to enhance the physical and mechanical properties. Throughout this paper this is referred to as the "crosslinking agent." Aspen wood veneer (provided by a local supplier) was used for the lap shear model tests.

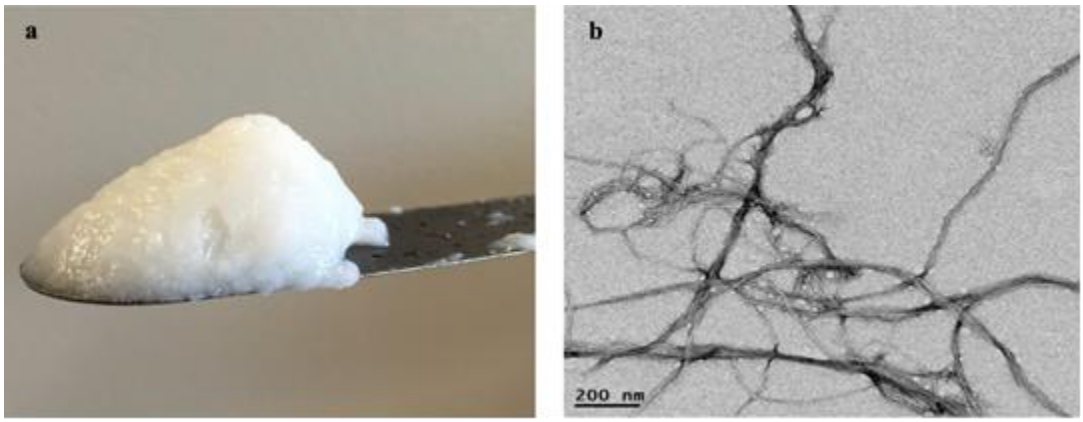

Fig. 1. Cellulose nanofibrils: (a) physical appearance of a 3 wt.% solids content slurry; and (b) TEM micrograph

Particleboard panels production

The WP with an average moisture content of 7% and CNF slurry at 3 wt.% solids were mixed at room temperature using a stand mixer. The mixture was then poured into a wooden forming box with the internal dimensions of 120 mm × 120 mm × 60 mm that was placed on top of a 40-mesh wire cloth. A wooden lid was placed on top, and a manual hydraulic press (Dake Corporation, Grand Haven, MI, USA) was used to press the mixture down and drain the excess water. Most of the free water was drained off during the cold pressing. The solids content of the mats before and after cold pressing were approximately 16% and 38%, respectively. This means that the cold pressing process was able to remove more than 50% of the water. Then the lid and forming box were removed and the cold pressed mat was pressed and dried using a hydraulic hot press (Carver, Inc., Wabash, IN, USA) at 180 °C for 7 min between two wire mesh cloths. Two metal stops 5-mm in thickness were used for position control. The particleboard panels were produced in four different groups of target density: 0.60 g cm-3 to 0.64 g cm^{-3} (group I), 0.65 g cm^{-3} to 0.69 g cm^{-3} (group II), 0.70 g cm^{-3} to 0.74 g.cm^{-3} (group III), and 0.75 g cm^{-3} to 0.79 g cm^{-3} (group IV). Each density group contained three samples of 15 wt.% and 20 wt.% dry CNF. After trimming, the final dimensions of each panel were 110 mm × 110 mm × 5mm. Each edge-trimmed panel was cut into three 110 mm × 30 mm specimens for the flexural tests. The production procedure is presented in Fig. 2.

To evaluate the effect of the addition of crosslinking agent on physical and mechanical properties, 85 wt.% WP and 15 wt.% CNF slurry (dry basis) were mixed at room temperature and 3 pph by weight, *i.e.* 3% of the total weight of the WP and CNF slurry mixture, crosslinking agent was added to the mixture. Panels with the crosslinking

agent added with the final edge-trimmed dimensions of 110 mm × 110 mm × 5 mm and the target density of 0.65 g cm^{-3} were made along with the control panels in the same manner explained above.

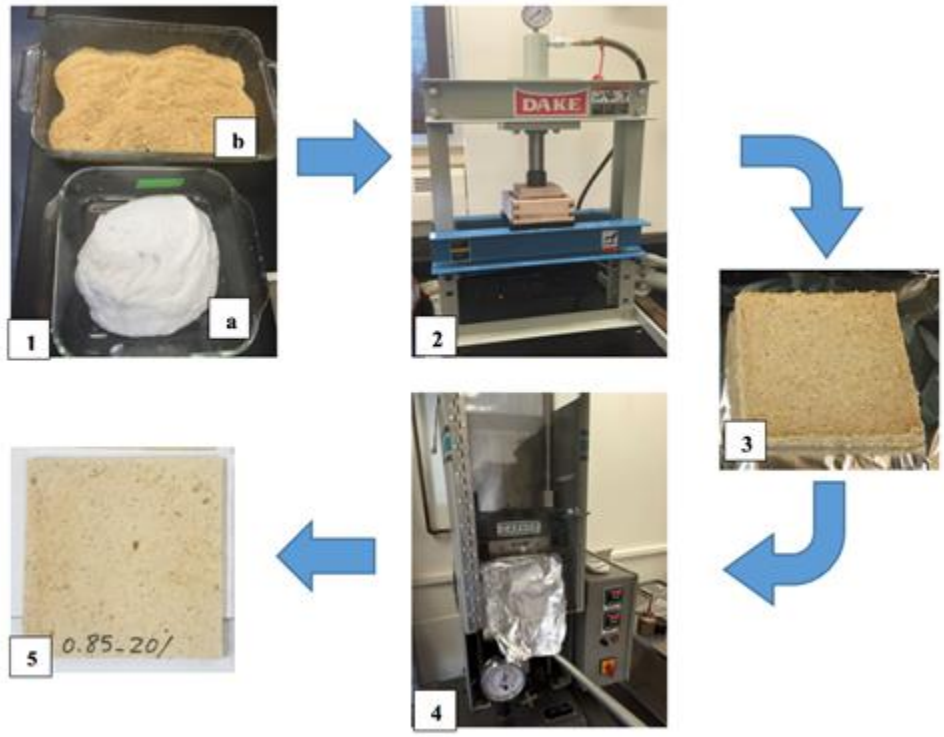

Fig. 2. PB panel production procedure: (1) raw materials: (a) 3 wt.% CNF slurry and (b) southern pine WP; (2) forming and cold pressing; (3) cold-pressed mat; (4) hot pressing; and (5) final panel

Methods

Evaluation of mat strength development

The WP and CNF slurry were mixed at a dry weight basis ratio of 7 to 3 at room temperature. Then the mixture was poured into a cylindrical mold and was pressed down by a manual hydraulic press (Dake Corp., Grand Haven, MI, USA) to partially drain and form into a wet disk. Five disk-shaped specimens with the nominal diameter of 45 mm and nominal height of 15 mm were made for the strength development test.

The disk-shaped samples were weighed after production. Then they were oven-dried at 120 °C. Every 15 min they were removed, weighed, and returned to the oven until fully dried. The moisture content (MC %) of the specimens was measured based on the weight of the specimens at each drying level and the oven-dry weight as follows,

$$MC\ (\%) = [(W\text{-}W_o) / W_o] \times 100 \quad (1)$$

where W and W_o are measured weights (g) at each level of drying and the oven-dry weight, respectively. This data was used to construct drying curves to be used to correlate drying time to moisture content. To investigate the strength development of the adhesion between the WP and CNF, a compression test was conducted on the disk-shaped samples after 30, 60, 120, 150, 180, 240, and 300 min of oven-drying at 120 °C. Five disk-shaped specimens with a nominal diameter of 45 mm and nominal height of 15 mm were made for each level of drying. The compression test was performed at approximately 23 °C with the crosshead

speed of 5 mm/min using an Instron 5500R universal testing machine (Instron, Norwood, MA, USA) with a 10 kN capacity load cell.

Lap-shear bonding strength investigation

Rectangular strands of 35 mm × 20 mm were prepared from aspen wood veneer with an average thickness of 1.25 mm in the grain direction. Lap shear specimens were produced by overlapping two strands bonded together using the CNF slurry. The length of lap area was 20 mm. To investigate the effect of surface roughness on the wood-CNF bonding strength, 150-grit and 400-grit sandpapers were used to sand twenty strands (ten strands of each) at the lap area, with ten control strands not sanded. Therefore, five lap-shear specimens of each category were prepared and then oven-dried at 120 °C for an hour to be ready for the lap-shear tests. Adhesive lap shear strength tests were performed to determine the wood-CNF bonding strength. The lap shear test was conducted in accordance with ASTM D4896-01 (2016) with modification using an Instron 4202 (Instron, Norwood, MA, USA) with a 10 kN capacity load cell and the crosshead speed of 0.1 mm/min. This low crosshead speed was required to avoid premature failure of the specimens.

Evaluation of flexural properties

For the determination of the modulus of elasticity (MOE) and modulus of rupture (MOR), a three-point bending test was performed on each 110 mm × 30 mm specimen according to ASTM D1037 (2012) with modifications using an Instron 5966 universal testing machine (Instron, Norwood, MA, USA) with a 10 kN load cell capacity. The span length and the crosshead speed were 80 mm and 3 mm/min, respectively. Specimens were conditioned to approximately 23 °C and 50% RH for at least 48 h prior to testing.

Water absorption and thickness swelling evaluation

To investigate the water absorption and thickness swelling of the PB, rectangular specimens were cut out of the broken flexural samples (one specimen out of each broken sample). The specimens were 50-mm long, 30-mm wide, and 5-mm thick. The water absorption and thickness swelling of the PB specimens were measured in accordance with ASTM D1037 (method A: 2-plus-22-h submersion in water) (2012).

Density profile

The evaluation of density distribution through the thickness of PB panels was conducted using a QMS X-ray density profiler (model: QDP-01X, Quintek Measurement Systems, Inc., Knoxville, TN, USA).

Evaluation of internal bond

To evaluate the internal bond (IB) strength of the panels, tension tests perpendicular to the surface were performed according to the ASTM D1037 standard (2012) with modifications using an Instron 5500R universal testing machine with a 10 kN capacity load cell. The specimens with the nominal dimensions of 30 mm × 30 mm × 5 mm (thickness) were cut out of the broken flexural samples (one specimen out of each broken sample) and glued to aluminum test fixtures using hot melted glue. The testing was conducted at a cross-head speed of 0.4 mm/min.

SEM microscopy

For the scanning electron microscopy (SEM) imaging, all samples were placed on specimen mounts with double-sided carbon tape, and then grounded on all edges with

conductive silver paint. After drying, they were sputter-coated using a Cressington 108 auto sputter coater (Ted Pella, Inc., Redding, CA, USA) with 23 nm of gold-palladium. For a better understanding of the surface morphology of the WP mixed with CNF, scanning electron microscope (SEM) images of the southern pine particles and the particles mixed with 3 wt.% CNF suspension after drying were taken at 20 kV using an Amray 1820 SEM (Amray, Inc., New Bedford, MA, USA). The SEM imaging was also used to investigate the wood-CNF bonding at fractured areas of the lap shear specimens.

Statistical analysis of experimental data

All experimental data were statistically analyzed with IBM SPSS Statistics Version 23 (IBM Corp., Armonk, NY, USA,). The mechanical and physical properties were statistically compared using two-way ANOVA tests. Duncan's multiple range test (DMRT) was used to evaluate the group means. A t-test was performed to evaluate the effect of the crosslinking agent as an additive. Comparisons were made based on a 95% confidence interval.

RESULTS AND DISCUSSION

Mechanical and Physical Properties

As expected, it was observed that the density has a considerable effect on the MOR and MOE of the panels. Changing the CNF content of the panels from 15% to 20% did not significantly (p-value = 0.388) change the MOE but increased the MOR values significantly (p-value = 0.003). The effect of the density of the produced PB on MOR and MOE for the panels that contained 15% and 20% CNF is illustrated in Fig. 3. This shows that the MOR and MOE increased with an increase in the density of the panels.

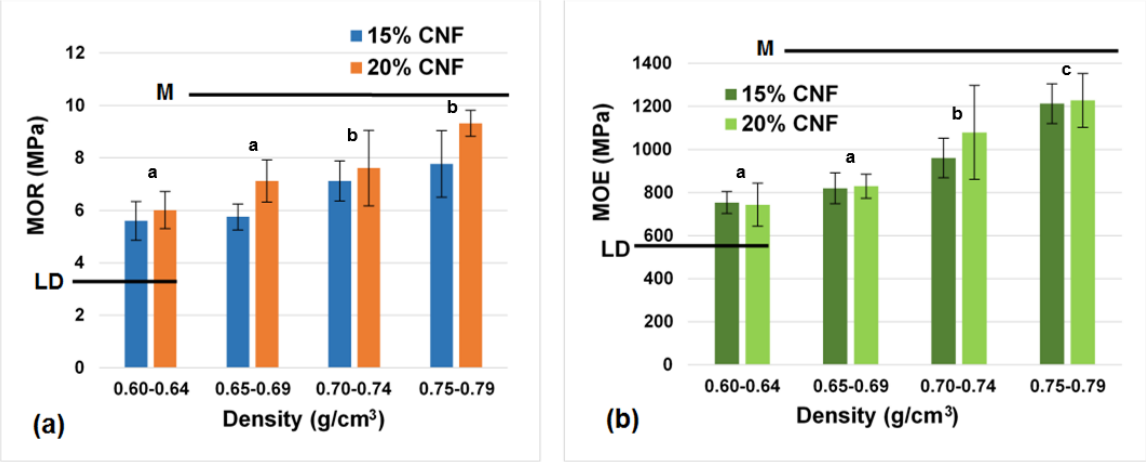

Fig. 3. Mechanical properties of 15% and 20% CNF-containing panels: (a) MOR (b) MOE. Columns with different letters are significantly different at a significance level of 0.05.

The DMRT test showed that the MOR values of the two lowest density levels were not significantly different from each other (p-value = 0.188). The same was true for the MOR of the two highest density levels (p-value = 0.064). The MOE of the two lowest density levels were not significantly different (p-value = 0.113), whereas all other density levels showed a statistically (p-value = 0.000) different effect on MOE. As mentioned

above, the CNF content did not meaningfully improve MOE, but did so for MOR. This could have been related to the fact that MOE of the panel mainly depended on the elastic moduli of both the WP and CNF. As the moduli of elasticity of CNF particles and southern pine wood are almost similar (Southern Pine Inspection Bureau 2013; Zhang *et al.* 2013), increasing the proportion of CNF in the formulation of the panel means decreasing the proportion of the WP, and consequently not noticeably altering the overall value of the MOE. In contrast, the MOR relates to the bonding strength of the adhesive. Therefore, increasing the proportion of CNF as a binder would result in an increase in MOR values.

The lines marked with M and LD in Fig. 3 represent the minimum required MOR and MOE for the medium-density and low-density particleboard panels, respectively, based on ANSI A208.1 (2016). As shown in Fig. 3, the produced panels fulfilled the requirements of the MOR and MOE standard levels for the low-density (less than 0.64 g cm^{-3}) particleboard panels. However, these values were lower than the minimum standard levels of both properties for the medium-density (generally between 0.64 g cm^{-3} to 0.8 g cm^{-3}) panels. To meet the M level requirements, several changes could be made to the PB configuration, such as using larger particles in the core layers and smaller ones in the surface layers. A three-layer layup with higher densities for the panel surfaces as opposed to a one-layer layup is common in the industrial particleboard manufacturing process.

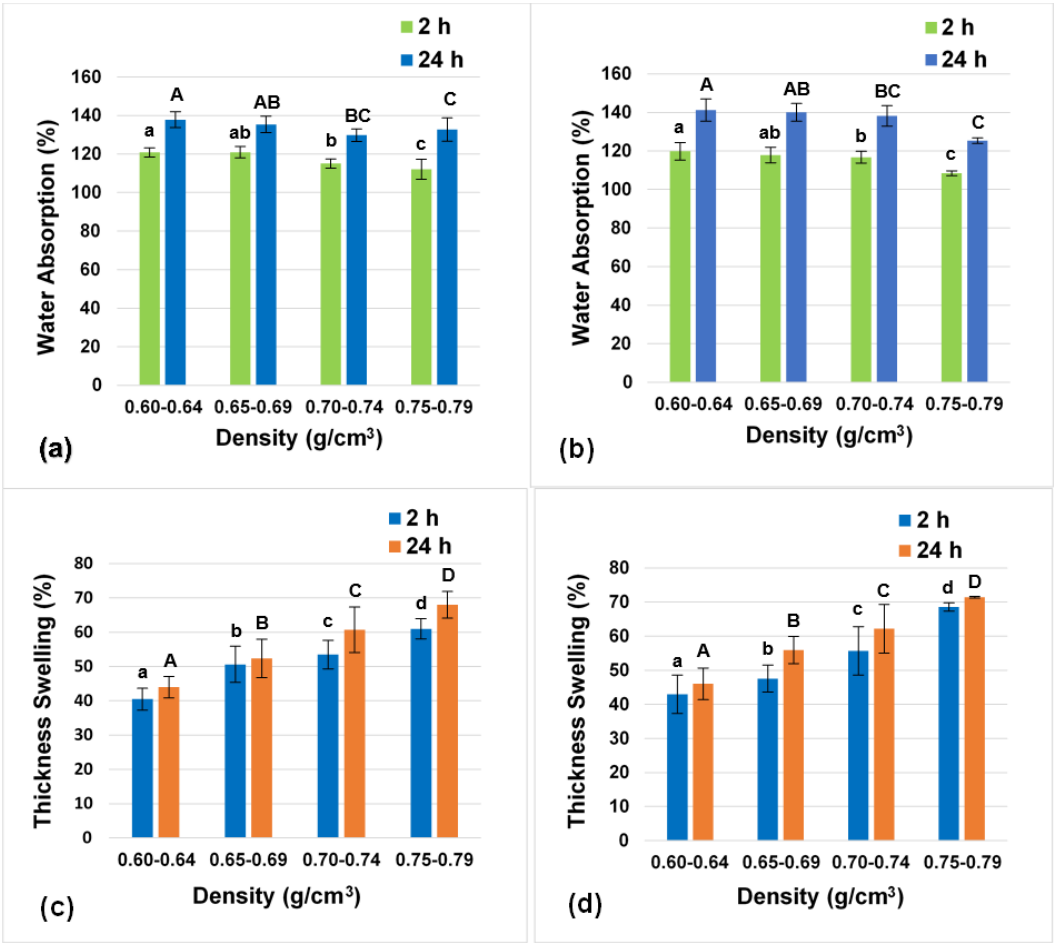

Fig. 4. Water absorption of (a) 15% and (b) 20% CNF containing panels; thickness swelling of (c) 15% and (d) 20% CNF-containing panels. Columns with different letters are significantly different at a significance level of 0.05.

Water absorption and thickness swelling properties of the produced panels were observed to be affected by the changes in density. However, there was no significant difference between panels that contained 15% and 20% CNF in terms of water absorption and thickness swelling, respectively. Figure 4 presents the results of water absorption and thickness swelling tests for the panels that contained 15% and 20% CNF after 2 h and 24 h of submersion, respectively. It can be seen that for all of the samples, most of the water was absorbed in the first 2 h of submersion. The DMRT test showed that the thickness swelling values after 2 h and 24 h of submersion were significantly (p-value = 0.000) different for all four density levels. However, the water absorption values after 2 h of submersion were not significantly different for the two lowest density levels (p-value = 0.573). The same was true for the second and third level of density (p-value = 0.054). Overall, with increased densities of the panels, the thickness swelling increased while an inverse effect on water absorption was observed. This was attributed to the packing density of the panel structures. As the density of panels increased (at a constant volume), the structure became more packed. Therefore, the number of pores through which water molecules diffuse decreased, which resulted in water absorption reduction. This is why the water absorption decreased with an increase in the density of panels. However, thickness swelling, increased as the density increased because the number of particles and binders swollen in a constant volume of panel increased with an increase in the density.

Despite considerable thickness swelling and water absorption of panels, all specimens maintained their integrity after the tests were completed. This was an encouraging observation for future research to focus on how low-density insulating panels could have high dimensional stability. It should be mentioned that thickness swelling and water absorption are not limiting factors for interior-grade particleboard panels in the U.S. (ANSI A208.1-2016 (2016)), but tests results are helpful in understanding bonding efficiency.

Effects of Adding a Crosslinking Agent

The addition of the crosslinking agent to the PB formulation altered the mechanical and physical properties of the panels. Results of flexural tests on both crosslinking agent- and non-crosslinking agent-added panels with the density of 0.65 $g.cm^{-3}$ are presented in Figs. 5a and b. It is shown that adding 3 pph of the crosslinking agent to the PB formulation almost doubled the MOR of the produced panels. It also caused the MOE of the panels to become nearly 1.5 times higher. In fact, the crosslinking agent used in this work was an aqueous solution of polyamidoamine-epichlorohydrin (PAE) resin, which had an azetidinium group (the cationic four-membered ring structure shown schematically in Fig. 6a) that could be cross-linked with the carboxyl groups (Fig. 6b) on the cellulosic structure of CNF and impart wet-strengthening on the PB structure (Li *et al.* 2004; Zhang *et al.* 2012).

The results of water absorption and thickness swelling testing performed on the crosslinking agent- and non-crosslinking agent-added specimens (Figs. 5c and d) indicated that the addition of the crosslinking agent to the PB formulation dramatically reduced the water absorption and thickness swelling of the panels, which was desirable for particleboard manufacturing. It was shown that the addition of the crosslinking agent decreased the thickness swelling amount by more than half. This was attributable to the fact that the reaction between the azetidinium functional group in the crosslinking agent structure and carboxylic groups in CNF results in a water-insoluble network (Li *et al.* 2004; Zhang *et al.* 2012).

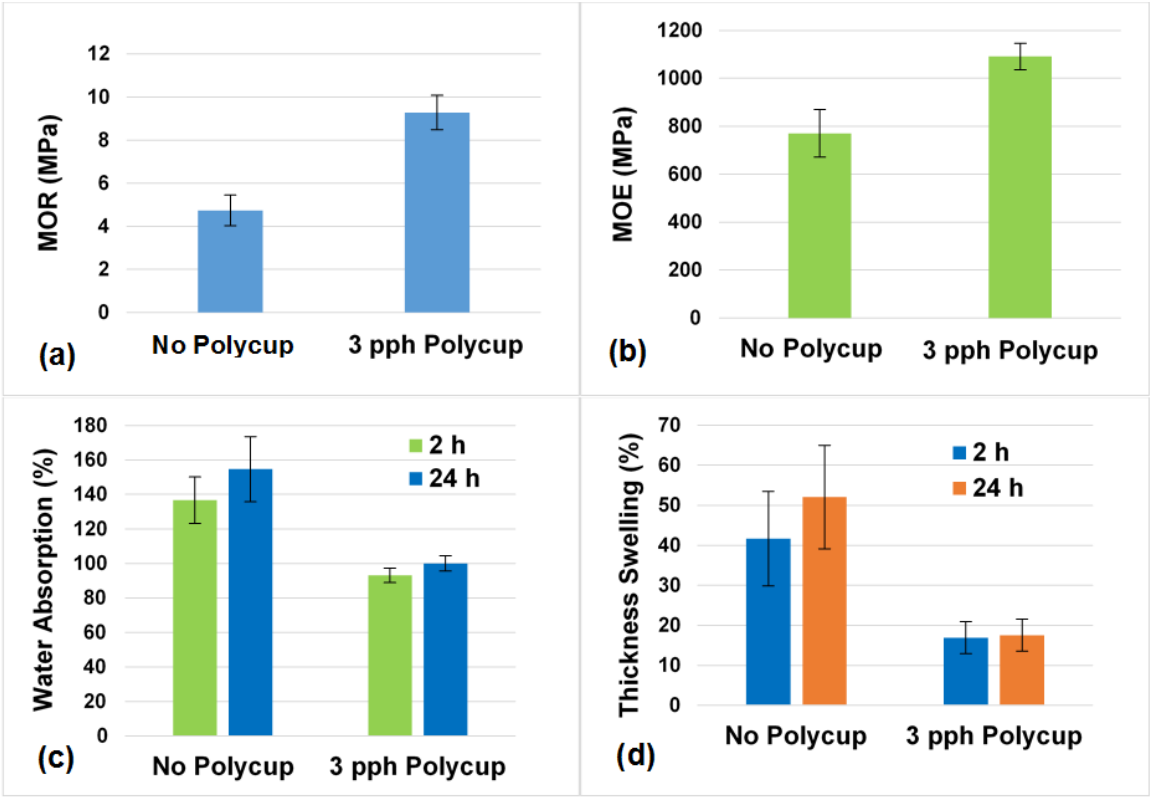

Fig. 5. Comparison of (a) MOR, (b) MOE, (c) water absorption, and (d) thickness swelling of panels with and without crosslinking agent

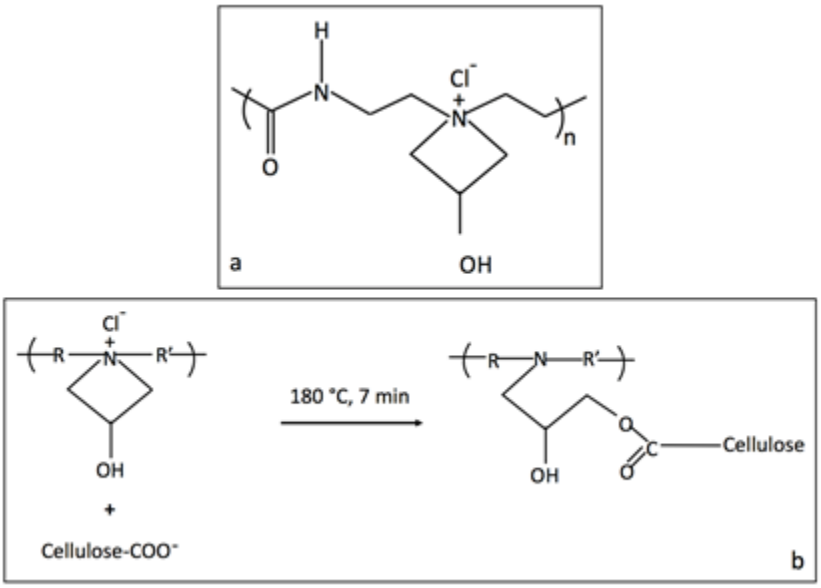

Fig. 6. (a) Scheme of chemical structure of PAE resins; (b) Reaction between the azetidinium groups of Polycup™ 5233 and carboxyl groups of bleached cellulose

Density Profile

The density profile analysis revealed that all produced PB panels had a U-shaped vertical density profile, which confirmed the higher density in the panel surfaces compared to the core. Density gradients are common in particleboards and can be favorable or

unfavorable, depending on their application. While a vertical density gradient can help increase flexural properties without increasing density, the performance of edge gluing and fastening is reduced as a result. Differences in density occur because of the differential heat transfer from the press platens that result in greater densification in the mat surfaces than in the core. If a curable resin is involved, this means that the faces are cured and set at a higher pressure while the core is still curing and sustaining the pressure (Wong *et al.* 1999). In the particular system presented in the current paper, no curing happened and all bonding took place when the CNF dried. Figure 7 shows the vertical density profiles of two PB panels with different mean density (MD) levels. It was observed that the difference between the surface and core densities was more noticeable at higher mean density levels due to the additional mass undergoing the pressure and heat.

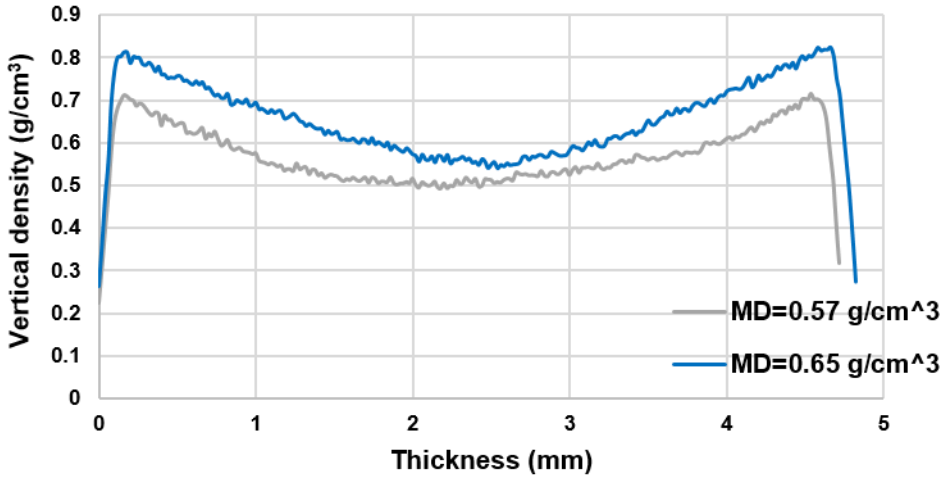

Fig. 7. Density profile of PB panels at two different mean density levels

Internal Bond

The results of the IB tests for the different groups of density and at CNF levels of 15% and 20% are shown in Fig. 8.

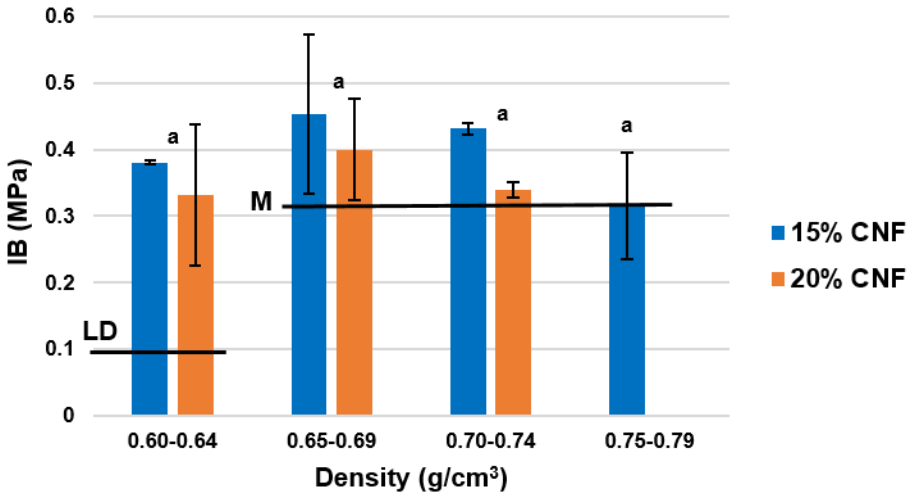

Fig. 8. Internal bond strength of 15% and 20% CNF containing panels. Columns with the same letters are not significantly different at a significance level of 0.05.

The IB values for the density group of 0.75 g cm^{-3} to 0.79 g cm^{-3} at 20% CNF level were not provided due to unacceptable failure during the test. The DMRT test showed that the IB values of all four groups of density (*p*-value = 0.103), and two different CNF levels (*p*-value = 0.128), were not significantly different. This was attributed to the relatively small differences in the core densities of all the panels observed in the density profile analysis. The lines marked with M and LD in Fig. 8 represent the minimum IB strength for the medium-density and low-density particleboard panels, respectively, based on ANSI A208.1 (2016). As shown in Fig. 8, the produced panels almost met the requirements of IB strength for both low-density and medium-density particleboard panels.

Strength Development

Drying time was a key factor in the strength development of the adhesion between the CNF and WP. The relationship between drying time and moisture content (MC %) of the disk-shaped samples was first studied. For all samples the moisture content levelled off after approximately 250 min of drying. This information was used to determine the drying time intervals needed to achieve the desired moisture contents for the strength development tests. Figure 9c shows the effect of the drying time on the strength development of the disk-shaped samples. As shown in Fig. 9d, the relationship between moisture content and compressive modulus of the disks was used as a measure for the strength development of the specimens.

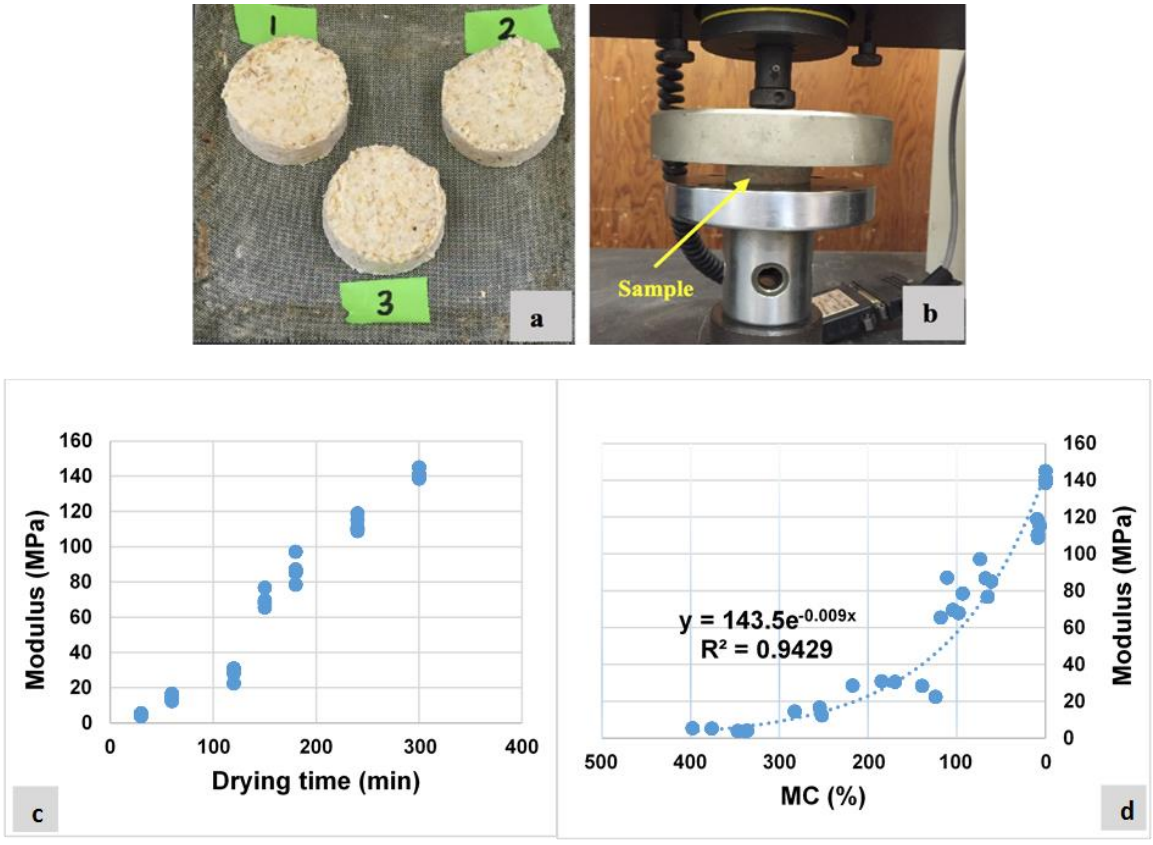

Fig. 9. (a) Disk-shaped samples used for strength development tests, (b) compression test set-up; Relationship between (c) drying time and modulus, (d) moisture content and compressive modulus of the disk-shaped samples

It was apparent that increased drying led to increased strength. This happens partly because of the hornification phenomenon, where the dewatering and drying of cellulose nanofibrils results in a strong bond between wood particles and cellulose nanofibrils. Furthermore, drying the samples until the fiber saturation point of wood (approximately 30% moisture content (Glass and Zelinka 2010)) should not substantially change the strength of the samples due to the removal of free water in wood particles and in the mat. However, drying the samples below the fiber saturation point increased the strength of the samples dramatically due to the removal of bound water in the cell wall of wood. It was also concluded that at approximately 10% moisture content, 90% of the maximum stiffness was achieved.

Bonding Strength and Mechanism

Results of the lap-shear tests (Fig. 10b) indicated that the surface roughness had a significant (p-value = 0.037) effect on the bonding strength. The 400-grit sanded strands had the strongest bond with the CNF, whereas strands that were not sanded had the least bonding strength. These findings corresponded to more microgrooves in the smoother surface that grabbed more CNF and led to better mechanical interlocking. The SEM micrographs of the unsanded control and sanded strands, along with the fractured ones after the lap-shear test, are presented in Fig. 11. The SEM micrographs confirmed the higher number and also smaller microgrooves on the surface of the 400-grit sanded strands compared to the other strands. They also verified the presence of nanocellulose fibrils on the surface of the broken strands after lap-shear testing (Figs. 11b, d, and f). Visual observation of the fractured surfaces of the lap shear specimens showed that in all cases, regardless of the surface roughness, an adhesive failure had occurred. The CNF that was used as the adhesive to bond the two strands of wood was fully detached from one side of the specimen, which indicated that the bonding between the CNF and wood surface was not greater than the shear strength of the CNF film. That is why minimal CNF fiber can be seen on the fractured surfaces of the specimens in the SEM micrographs.

The CNFs at low solids content can be largely dispersed and exfoliated in water, and they can result in a three-dimensional network of fibrils upon drying. If wood particles are present in the system, the CNF particles can encompass particles mixed with them and hold them together upon water removal. Considering the exceptionally high mechanical properties of cellulose nanoparticles (Reising *et al.* 2013) and excellent hydrogen bonding between cellulose nanoparticles and other types of cellulosic materials (Joseleau *et al.* 2012), cellulose nanofibrils can bond wood particles to form a strongly bonded composite system. Figure 12a depicts a wet mat formed by mixing CNF suspension and wood particles. Such a system was composed of wood particles, CNF, water, and air. Upon dewatering and subsequent drying, a three-dimensional network of CNF was considered to form that held together the wood particles. At the micro/nano scale, it seemed that smaller particles of CNF could penetrate the porous structure of wood particles that provided strong bonds. Figure 12b and c demonstrate how wood particles can be bound together using CNF. Figure 12b shows the surface of a southern pine wood particle used in the production of the particleboard panels. The surface of a similar wood particle after being mixed with a CNF slurry and air-dried overnight is shown in Fig. 12c. The CNF fibrils were easily observed as distributed over the particle surface with some particles agglomerated into platelet shapes and some preserving their fibrillar morphology with varying fibril widths. It was thought that at least smaller parts of the CNF particles in the suspension would penetrate into the structures' pores and voids in the wood particles. Once the wood particles

with CNF surrounding them were in contact and hot pressed, a three-dimensional network of CNF fibrils formed and encompassed the particles in the panel structure, which gave it strength and stiffness. The strength of the bonds formed between two wood particles would depend on the degree to which the interpenetration of CNF was achieved, and the surface characteristics of the wood particles and CNF.

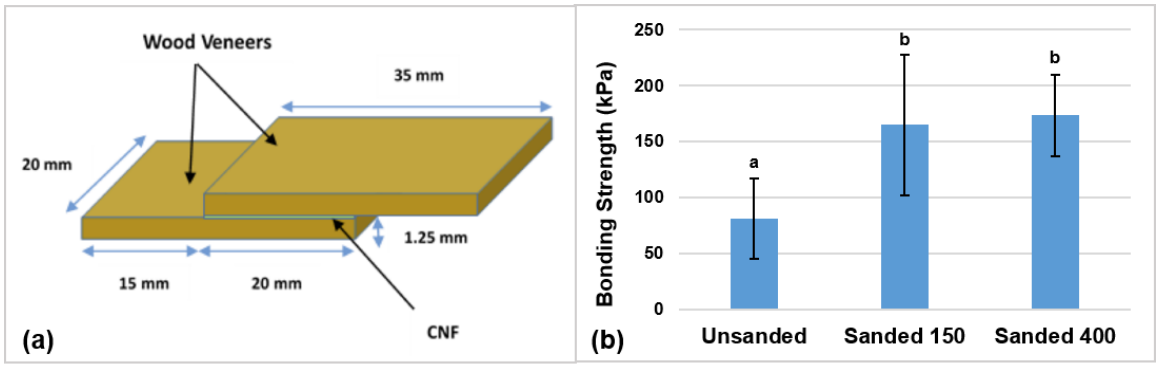

Fig. 10. (a) Schematic diagram of a lap-shear specimen; (b) Bonding strength of the lap shear specimens with different surface roughness (Columns with different letters were significantly different at a significance level of 0.05.)

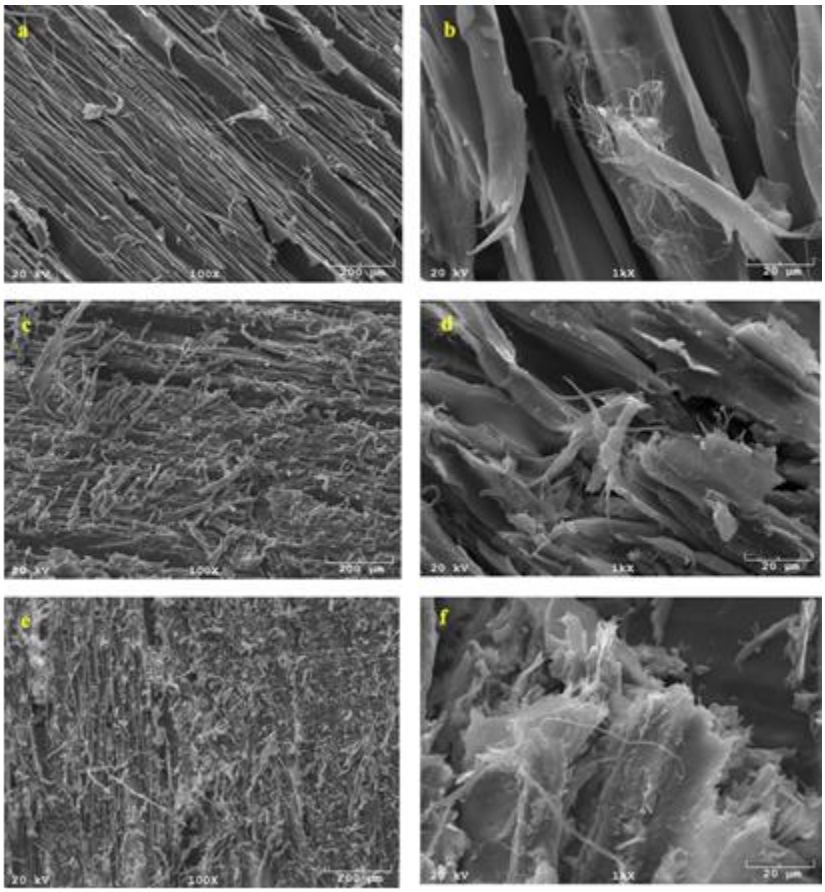

Fig. 11. SEM micrographs of the surface morphology of (a) unsanded control, (b) broken unsanded, (c) sanded 150 control, (d) broken sanded 150, (e) sanded 400 control, and (f) broken sanded 400 strands

The adhesion studies presented in this paper solely focused on the effect of mechanical interlocking and disregarded hydrogen bonding as a major contributor to bond strength (Gardner *et al.* 2008). The low values of lap shear strength observed in this study imply that hydrogen bonding would be the most important contributor to adhesion in the studied system (Gardner and Tajvidi 2016). The lap shear testing presented in this work may also not be representative of the bonding that happens in an actual wood particle-CNF system. In such a system, CNF can be assumed to encompass wood particles in a three dimensional network where CNF-CNF interactions might actually play a more important role than CNF-wood particle interactions (Fig. 12a). These interesting topics are the focus of the authors' current and future research.

The findings presented in this article provide a sound basis for a more focused effort on alternative applications of cellulose nanomaterials, particularly CNF as a binder in composite systems. However, the processing method presented in current paper to produce PB panels was different from that used for PB manufacturing on an industrial scale. For CNF to be used as binder in particleboard manufacturing, future research should be directed towards processes that minimize the amount of water in the mat to be pressed in the hot press. This calls for attaining a balance between the amount of water that can be tolerated in the press and that required for effective hydrogen bonding to occur.

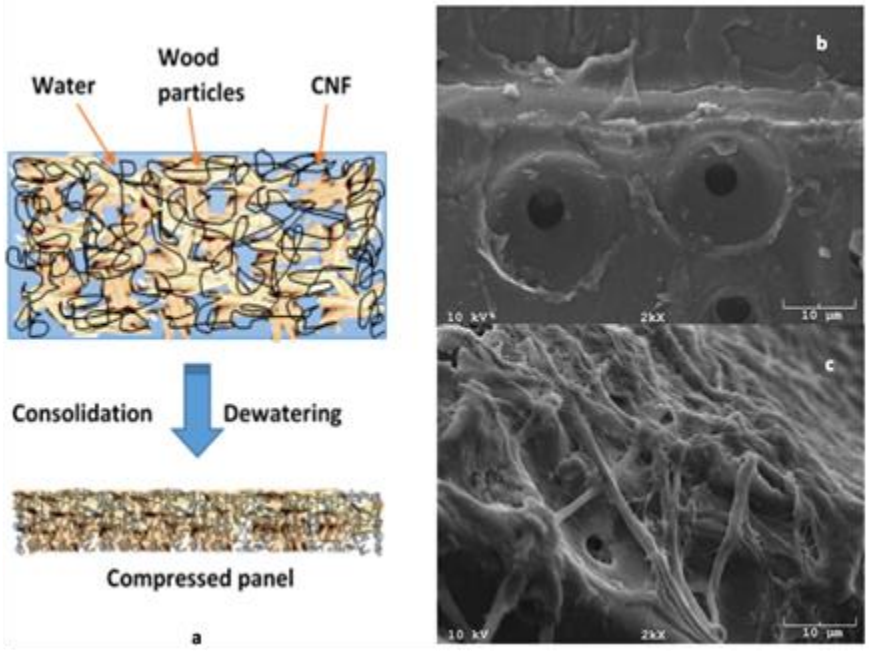

Fig. 12. (a) Consolidation and dewatering phenomenon followed by drying led to bond formation at micro/nano scale**;** SEM image of (b) the surface of a southern pine particle and (c) a southern pine particle mixed with a 3% solids content CNF after air-drying overnight.

CONCLUSIONS

1. The PB panels manufactured using CNF as the sole binder were shown to meet the industry requirements in terms of mechanical properties for low-density grades. The MOR and MOE of the produced panels increased with increased density levels.

2. The panel's density affected the water absorption and thickness swelling properties inversely. Water absorption decreased as the density of the panels increased. However, increased density led to an increase in the thickness swelling of the panels.
3. Moisture removal plays a major role in the strength development of the adhesion between WP and CNF.
4. The surface roughness had a significant effect on the strength of the WP-CNF bonding. The 400-grit sanded lap shear specimens had higher bonding strength values compared to the 150 grit sanded ones. The unsanded lap shear specimens had the weakest bonding strength.

ACKNOWLEDGMENTS

This project was funded by U. S. Endowment for Forestry and Communities, Inc. (P^3Nano) grant number P3-5. This project was supported by the USDA National Institute of Food and Agriculture, McIntire-Stennis project number # ME041616 through the Maine Agricultural & Forest Experiment Station. Maine Agricultural and Forest Experiment Station Publication Number MAFES #3527.

REFERENCES CITED

Amazio, P., Avella, M., Errico, M. E., Gentile, G., Balducci, F., Gnaccarini, A., Moratalla, J., and Belanche, M. (2011). "Low formaldehyde emission particleboard panels realized through a new acrylic binder," *J. Appl. Polym. Sci.* 122, 2779-2788. DOI: 10.1002/app

ANSI A208.1-2016 (2016). "Particleboard," American National Standard, Leesburg, VA.

Antonovic, A., Jambrekovic, V., Kljak, J., Spanic, N., and Medved, S. (2010). "Influence of urea-formaldehyde resin modification with liquefied wood on particleboard properties," *Drvna Industrija* 61(1), 5-14.

ASTM D1037-12 (2012). "Standard test methods for evaluating properties of wood-base fiber and particle panel materials," ASTM International, West Conshohocken, PA.

ASTM D4896-01 (2016). "Standard guide for use of adhesive-bonded single lap-joint specimen test results," ASTM International, West Conshohocken, PA.

Bertaud, F., Tapin-Lingua, S., Pizzi, A., Navarrete, P., and Petit-Conil, M. (2012). "Development of green adhesives for fiberboard manufacturing, using tannins and lignin from pulp mill residues," *Cell. Chem. Technol.* 46(7-8), 449-455.

Bilodeau, M. A., and Bousfield, D. W. (2014). "Composite building products bound with cellulose nanofibers," U. S. Patent No. US 20150033983 A1.

Charreau, H., Foresti, M. L., and Vázquez, A. (2013). "Nanocellulose patents trends: A comprehensive review on patents on cellulose nanocrystals, microfibrillated and bacterial cellulose," *Recent Pat. Nanotechnol.* 7(1), 56-80.

Chirayil, C. J., Mathew, L., and Thomas, S. (2014). "Review of recent research in nanocellulose preparation from different lignocellulosic fibers," *Rev. Adv. Mater. Sci.* 37, 20-28.

Christensen, R., Robitschek, P., and Stone, J. (1981). "Formaldehyde emission from particleboard," *Holz Als Roh-Und Werkstoff* 39(6), 231-234.

Dufresne, A. (2012). *Nanocellulose: From Nature to High Performance Tailored Materials*, Walter de Gruyter, Berlin.

Elbert, A. A. (1995). "Influence of hardener systems and wood on the formaldehyde emission from urea-formaldehyde resin and particleboards," *Holzforschung* 49(4), 358-362.

Gardner, D. J., Blumentritt, M., Kiziltas, A., Kiziltas, E. E., Peng, Y., and Yildirim, N. (2013). "Polymer nanocomposites from the surface energy perspective," *Rev. Adhes. Adhes*. 1(2), 175-215. DOI: https://doi.org/10.7569/RAA.2013.097309

Gardner, D. J., Oporto, G. S., Mills, R., and Samir, M. A. S. A. (2008). "Adhesion and surface issues in cellulose and nanocellulose," *J. Adhes. Sci. Technol.* 22, 545-567. DOI: 10.1163/156856108X295509

Gardner, D. J., and Tajvidi, M. (2016). "Hydrogen bonding in wood-based materials: An update," *Wood Fiber Sci.* 48(4), 1-11.

Glass, V. S., and Zelinka, S. L. (2010). "Moisture relations and physical properties of wood," in: *Wood handbook: Wood as an Engineering Material* (Centennial Ed.), Forest Products Laboratory, United States Department of Agriculture Forest Service, Madison, WI.

Hubbe, M. A., Rojas, O. J., Lucia, L. A., and Sain, M. (2008). "Cellulosic nanocomposites: A review," *BioResources* 3(3), 929-980.

Ince, P. J. (1999). "Global cycle changes the rules for U.S. pulp and paper," *PIMA's North American Papermaker* 81(12), 37-42.

Jambrekovi, V., Brezovi, M., Kljak, J., and Antonovi, A. (2006). "Development options of composite materials from wood particles in the Republic of Croatia," *Drvna Industrija* 57(4), 183-191.

Joseleau, J. P., Chevalier-Billosta, V., and Ruel, K. (2012). "Interaction between microfibrillar cellulose fines and fibers: Influence on pulp qualities and paper sheet properties," *Cellulose* 19(3), 769-777. DOI: 10.1007/s10570-012-9693-5

Klemm, D., Kramer, F., Moritz, S., Lindström, T., Ankerfors, M., Gray, D., and Dorris, A. (2011). "Nanocelluloses: A new family of nature based materials," *Angew. Chem. Int.* 50(24) 5438-5466. DOI: 10.1002/anie.201001273

Kojima, Y., Ishino, A., Kobori, H., Suzuki, S., Ito, H., Makise, R., Higuchi, I., and Okamoto, M. (2015). "Reinforcement of wood flour board containing ligno-cellulose nanofiber made from recycled wood," *J. Wood Sci.* 61, 492-499. DOI: 10.1007/s10086-015-1493-8

Kojima, Y., Minamino, J., Isa, A., Suzuki, S., Ito, H., Makise, R., and Okamoto, M. (2013). "Binding effect of cellulose nanofibers in wood flour board," *J. Wood Sci.* 59, 396-401. DOI: 10.1007/s10086-013-1348-0

Li, K., Peshkova, S., and Geng, X. (2004). "Investigation of soy protein-Kymene® adhesive systems for wood composites," *J. Amer. Oil Chem. Soci.* 81(5), 487-491. DOI: 10.1007/s11746-004-0928-1

Moon, R. J., Martini, A., Nairn, J., Simonsen, J., and Youngblood, J. (2011). "Cellulose nanomaterials review: Structure, properties and nanocomposites," *Chem. Soc. Rev.* 40(7), 3941-3994. DOI: 10.1039/C0CS00108B

Oksman, K., Aitomäki, Y., Mathew, A. P., Siqueira, G., Zhou, Q., Butylina, S., Tanpichai, S., Zhou, X., and Hooshmand, S. (2016). "Review of the recent

developments in cellulose nanocomposite processing," *Compos. Part A-Appl. S.* 83, 2-18. DOI: http://dx.doi.org/10.1016/j.compositesa.2015.10.041

Prasittisopin, L., and Li, K. (2010). "A new method of making particleboard with a formaldehyde-free soy-based adhesive," *Compos. Part A- Appl. S.* 41, 1447-1453. DOI: http://dx.doi.org/10.1016/j.compositesa.2010.06.006

Prestemon, J. P., Wear, D. N., and Foster, M. O. (2015). "The global position of the U.S. forest products industry," e-Gen. Tech. Rep. SRS-204. Asheville, NC: U.S. Department of Agriculture Forest Service, Southern Research Station. 24 p.

Reising, A. B., Moon, R. J., and Youngblood, J. P. (2013). "Effect of particle alignment on mechanical properties of neat cellulose nanocrystal films," *J. Sci. Technol. Forest Prod. Process.* 2(6), 32-41.

Seyno, W. C., Creamer, A. W., Wu, C. F., and Lora, J. H. (1996). "The use of organosolv lignin to reduce press vent formaldehyde emissions in the manufacture of wood composites," *Forest Prod. J.* 46(6), 73-77.

Siró, I., and Plackett, D. (2010). "Microfibrillated cellulose and new nanocomposite materials: A review," *Cellulose* 17(3), 459-494. DOI: 10.1007/s10570-010-9405-y

Sivasubramanian, S., Reynaud, E., and Schmidt, D. (2009). *Alternative Formaldehyde-free Particleboard Compositions Based on Epoxidized Vegetable Oils*, University Research in Sustainable Technologies Program, University of Massachusetts Lowell, Lowell, MA.

Southern Pine Inspection Bureau (2013). Supplement No. 13 to the southern pine inspection bureau grading rules 2002 edition, (http://www.spib.org/pdfs/SupplementNo13RevisedFebruary11.pdf), Accessed 1 September 2016.

Tajvidi, M., Gardner, D. J., and Bousfield, D. (2016). "Cellulose nanomaterials as binders: Laminate and particulate systems," *J. Renew. Mater.* 4(5), 365-376. DOI: https://doi.org/10.7569/JRM.2016.634103

Tasooji, M., Tabarsa, T., Khazaeian, A., and Wool, R. P. (2010). "Acrylated epoxidized soy oil as an alternative to urea-formaldehyde in making wheat straw particleboards," *J. Adhes. Sci. Technol.* 24(8-10), 1717-1727. DOI: 10.1163/016942410X507786

Theng, D., Arbat, G., Delgado-Aguilar, M., Vilaseca, F., Ngo, B., and Mutjé, P. (2015). "All-lignocellulosic fiberboard from corn biomass and cellulose nanofibers," *Ind. Crops Prod.* 76 (2015), 166-173. DOI: http://doi.org/10.1016/j.indcrop.2015.06.046

Tongboon, S., Kiatkamjornwong, S., Prasassarakich, P., and Oonjittichai, W. (2002). "Particleboard from rubber wood flakes with polymeric MDI binder," *Wood Fiber Sci.* 34(3), 391-397.

Veigel, S., Rathke, J., Weigl, M., and Gindl-Altmutter, W. (2012). "Particle board and oriented strand board prepared with nanocellulose-reinforced adhesive," *J. Nanomater.* 2012, 1-8. DOI: 10.1155/2012/158503

Wong, E. D., Zhang, M., Wang, Q., and Kawai, S. (1999). "Formation of the density profile and its effects on the properties of particleboard," *Wood Sci. Technol.* 33(4), 327-340. DOI: 10.1007/s002260050119

Xing, S., Riedl, B., Deng, J., Nadji, H., and Koubaa, A. (2013). "Potential of pulp and paper secondary sludge as co-adhesive and formaldehyde scavenger for particleboard manufacturing," *Euro. J. Wood Prod.* 71(6), 705-716. DOI: 10.1007/s00107-013-0729-9

Zhang, W., Zhang, Y., Lu, C., and Deng, Y. (2012). "Aerogels from crosslinked cellulose nano/micro-fibrils and their fast shape recovery property in water," *J. Mater. Chem.* 22, 11642-11650. DOI: 10.1039/C2JM30688C

Zhang, Y., Nypelo, T., Salas, C., Arboleda, J., Hoeger, I. C., and Rojas, O. J. (2013). "Cellulose nanofibrils: From strong materials to bioactive surfaces," *J. Renew. Mater.* 1(3), 195-211. DOI: 10.7569/JRM.2013.634115

Article submitted: February 2, 2017; Peer review completed: March 30, 2017; Revised version received and accepted: April 10, 2017; Published: April 24, 2017.
DOI: 10.15376/biores.12.2.4093-4110